High-affinity lamprey VLRA and VLRB monoclonal antibodies

Citation: Tasumi, Satoshi et al. "High-affinity lamprey VLRA and VLRB monoclonal antibodies." Proceedings of the National Academy of Sciences 106.31 (2009): 12891-12896. © 2009 National Academy of Sciences

As Published: http://dx.doi.org/10.1073/pnas.0904443106

Publisher: United States National Academy of Sciences

Persistent URL: http://hdl.handle.net/1721.1/52559

Version: Final published version: final published article, as it appeared in a journal, conference proceedings, or other formally published context

High-affinity lamprey VLRA and VLRB monoclonal antibodies

Satoshi Tasumi[a], C. Alejandro Velikovsky[b], Gang Xu[a], S. Annie Gai[c], K. Dane Wittrup[c], Martin F. Flajnik[d], Roy A. Mariuzza[b], and Zeev Pancer[a,1]

[a]Center of Marine Biotechnology, University of Maryland Biotechnology Institute, Baltimore, MD 21202; [b]Center for Advanced Research in Biotechnology, W.M. Keck Laboratory for Structural Biology, University of Maryland Biotechnology Institute, Rockville, MD 20850; [c]Department of Chemical Engineering and Department of Biological Engineering and Koch Institute for Integrative Cancer Research, Massachusetts Institute of Technology, Cambridge, MA 02139; and [d]Department of Microbiology and Immunology, University of Maryland at Baltimore, Baltimore, MD 21201

Edited by Max D. Cooper, Emory University, Atlanta, GA, and approved June 16, 2009 (received for review April 22, 2009)

Lamprey are members of the ancestral vertebrate taxon (jawless fish), which evolved rearranging antigen receptors convergently with the jawed vertebrates. But instead of Ig superfamily domains, lamprey variable lymphocyte receptors (VLRs) consist of highly diverse leucine-rich repeats. Although VLRs represent the only known adaptive immune system not based on Ig, little is known about their antigen-binding properties. Here we report robust plasma VLRB responses of lamprey immunized with hen egg lysozyme and β-galactosidase (β-gal), demonstrating adaptive immune responses against soluble antigens. To isolate monoclonal VLRs, we constructed large VLR libraries from antigen-stimulated and naïve animals in a novel yeast surface-display vector, with the VLR C-terminally fused to the yeast Flo1p surface anchor. We cloned VLRB binders of lysozyme, β-gal, cholera toxin subunit B, R-phycoerythrin, and B-trisaccharide antigen, with dissociation constants up to the single-digit picomolar range, equivalent to those of high-affinity IgG antibodies. We also isolated from a single lamprey 13 anti-lysozyme VLRA clones with affinities ranging from low nanomolar to mid-picomolar. All of these VLRA clones were closely related in sequence, differing at only 15 variable codon positions along the 244-residue VLR diversity region, which augmented antigen-binding affinity up to 100-fold. Thus, VLRs can provide a protective humoral antipathogen shield. Furthermore, the broad range of nominal antigens that VLRs can specifically bind, and the affinities achieved, indicate a functional parallelism between LRR-based and Ig-based antibodies. VLRs may be useful natural single-chain alternatives to conventional antibodies for biotechnology applications.

adaptive immunity | agnatha | somatic rearrangement

Jawed vertebrates, such as sharks, birds, and mammals, mount a robust humoral response on immune stimulation with foreign antigens. Typically, naïve B lymphocytes bind antigens with low affinity via surface IgM. Subsequently, antibody genes undergo somatic hypermutation, and those clones with highest affinity are selected to produce effective immune responses and form the memory pool (1, 2). Lamprey and hagfish are jawless fish, representatives of the ancestral vertebrate taxon, which evolved rearranging antigen receptors convergently with the jawed vertebrates. But instead of the Ig superfamily domains found in Ig-based antibodies and T cell receptors (TCRs), the variable lymphocyte receptors (VLRs) of lamprey and hagfish consist of highly diverse leucine-rich repeat (LRR) modules (3–6). LRRs are ancient protein modules that are prevalent building blocks of animal and plant pattern recognition molecules, such as Toll and Toll-like receptors, nucleotide oligomerization domain (NOD) LRRs, and plant disease-resistance genes, which are triggered by an exceptionally diverse array of ligands (7). Interestingly, however, VLRs are not related to these pattern recognition molecules, but instead are closely related to the vertebrate-specific von Willebrand factor receptor GpIbα, a member of the family of platelet LRR-containing hemostatic receptors (6). Jawless vertebrates thus evolved their rearranging antigen receptors from LRR scaffolds, elaborating the only known adaptive immune system not based on Ig or on TCR (6). But little is known about the antigen-binding properties of VLRs, or about how the naïve VLR repertoire develops into a protective shield in immune-stimulated animals.

There are 2 types of VLR genes (4, 6), *VLRA* and *VLRB*, expressed by mutually exclusive lymphocyte populations (8). To form mature functional receptors, germline VLR genes undergo DNA recombination, whereby each VLR is assembled from multiple LRR-encoding cassettes selected from arrays of several hundred cassettes flanking each VLR gene. Mature VLRs consist of N-terminal leaders and C-terminal stalk-like cell surface–anchoring domains encoded by the germline VLR genes. Each VLR has a unique diversity region. Only small amino- and carboxy-terminal portions of the diversity regions are contributed by the germline genes (Fig. S1); these serve as docking sites for the sequential incorporation of LRR cassettes via a gene conversion–like process (6, 9).

The diversity regions in VLRA and VLRB consist of sets of LRR modules, each with a highly variable sequence: a 27- to 34-residue N-terminal LRR (LRRNT), one 25-residue LRR (LRR1), up to nine 24-residue LRRs (LRRVs; the terminal one designated LRRVe), one 16-residue truncated LRR designated the connecting peptide (CP), and a 48- to 63-residue C-terminal LRR (LRRCT). The LRRNT and LRRCT are stabilized by 2 sets of intramodular disulfide bonds that serve to cap both ends of the curved, solenoid-shaped diversity region (10). The assembly of VLRs by iterated cassette insertions, with frequent recombination events within boundaries of the LRR modules, generates a vast repertoire of receptors estimated at more than 10^{14} unique VLRs, of comparable magnitude to mammalian antibodies and TCRs (5, 6). Thus, VLRs may be excellent single-chain alternatives to Ig-based antibodies for biotechnology applications, because both antigen receptors were optimized over hundreds of millions of years of evolution.

Recent evidence indicates antigen recognition by plasma VLRB from immunized lamprey. Within 4–8 weeks after i.p. injection of *Bacillus anthracis* spores, the lamprey plasma contained VLRB antibodies that reacted specifically with the spores and with their BclA glycoprotein component (5, 11). Recombinant VLRBs from anthrax-immunized larvae were cloned and expressed in a mammalian cell line. Some of these could discriminate between the C-terminal domain of BclA of *B. anthracis* and *B. cereus*, which differ by only 14 of 134 residues, indicating the high specificity that VLRs can achieve. Both plasma VLRB and the recombinant

Author contributions: S.T., K.W., M.F., R.A.M., and Z.P. designed research; S.T., C.A.V., G.X., A.G., M.F., and Z.P. performed research; Z.P. analyzed data; and Z.P. wrote the paper.

The authors declare no conflict of interest.

This article is a PNAS Direct Submission.

Data deposition: The sequences reported in this paper have been deposited in the GenBank database (accession nos. FJ794792–FJ794814 and FJ804413.)

[1]To whom correspondence should be addressed. E-mail: pancer@comb.umbi.umd.edu.

This article contains supporting information online at www.pnas.org/cgi/content/full/0904443106/DCSupplemental.

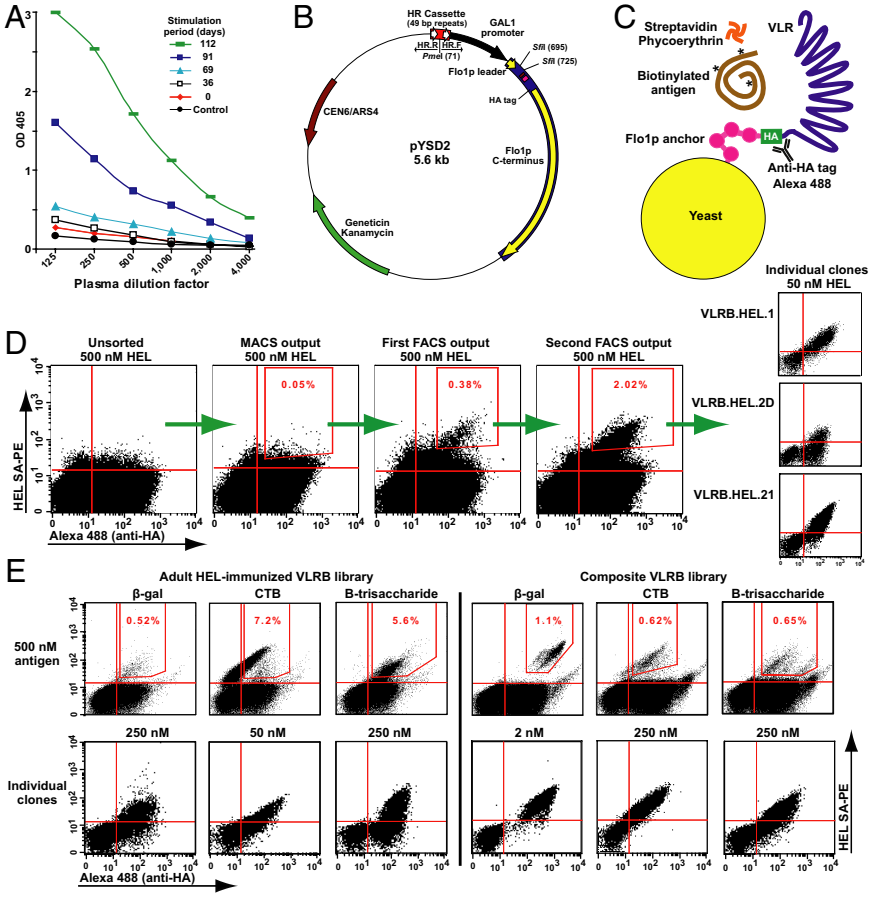

Fig. 1. Antigen binding by VLRB antibodies. (*A*) Plasma from HEL-immunized adult lamprey sampled and boosted as indicated. Direct ELISA with 1 μg/well of HEL, anti-VLRB mAb for detection, and streptavidin as a control. (*B*) The pYSD2 vector. VLR were directionally cloned in 2 different SfiI sites, between the Flo1p leader and C terminus, under control of the GAL1 promoter. An intraplasmid homologous recombination cassette consisted of two 49-nucleotide direct repeats separated by a *Pme*I restriction site, for plasmid linearization. Primers HR.F and HR.R served for rolling-circle amplification across the plasmid. (*C*) Yeast surface display of VLR fused to the Flo1p anchor. The HA-tag served for VLR detection via Alexa 488-conjugated antibodies. Biotinylated ligands were detected via SAPE. (*D*) Enrichment of HEL-binding VLRB clones from HEL-immunized larval library. From left to right: the unsorted library, enrichment by antibiotin magnetic microbeads (with MACS), sorting of the double-positive cells in the gate, output of the first sort, output of the second sort, and the resulting clones. (*E*). Comparison of naïve and immune YSD libraries enriched for binders of β-gal, CTB, and B-trisaccharide. A representative clone for each antigen is shown.

antianthrax antibodies formed multimers, comprising 4 or 5 disulfide-linked dimeric subunits, which avidly bound BclA. But monomeric forms of the antianthrax VLRB were weak BclA binders, indicating that high-avidity binding requires oligomerization (11). In another study, lamprey immunized to human blood group O erythrocytes produced anti–H-trisaccharide plasma VLRB, and the crystal structure of this complex was reported (12). But immunization with soluble antigens produced no measurable response, and thus it was concluded that the lamprey immune system is biased toward repetitive epitopes displayed by particulate antigens (8).

Here we describe the antigen-binding properties of lamprey VLRA and VLRB antibodies obtained from large VLR yeast surface display (YSD) libraries, which were constructed from antigen-stimulated and naïve animals. This powerful high-throughput platform enabled us to isolate monoclonal VLRs that specifically bind proteins and carbohydrates with affinities ranging from micromolar to subnanomolar. We also demonstrated in vitro affinity maturation of VLRB antibodies, with up to a 1,300-fold improvement in antigen-binding properties, and obtained evidence for possible in vivo affinity maturation of VLRA antibodies.

Results and Discussion

Immune Response to Soluble Antigens. To study the role of VLRB in lamprey immunity, we immunized an adult and larvae to hen egg lysozyme (HEL) (see *SI Materials and Methods*), a soluble monovalent antigen commonly used to study the antigen-binding properties of jawed vertebrate Ig-based antibodies (13, 14). For strong and persistent stimulation of lamprey immune responses, we used Freund's complete adjuvant (FCA) or heat-killed bacteria. Within 2–4 months, high-titer anti-HEL VLRB responses were evident in plasma from the immunized animals (Fig. 1*A*); larvae immunized with β-galactosidase (β-gal) responded similarly. These data provide bona fide evidence of the adaptive immune responses of lamprey against soluble antigens. Interestingly, ELISA assays with plasma VLRB from HEL-immunized lamprey showed strong reactivity only when HEL was coated onto the ELISA plate, likely due to avidity, but only weak signals when immobilized VLRB was reacted with soluble HEL. This further indicates that native multimeric VLRBs are high-avidity receptors that may have evolved to opsonize and neutralize invading pathogens akin to IgM antibodies (8, 11).

VLR Yeast Surface Display Platform. To access the lamprey VLR repertoire, we constructed a novel YSD vector (see *SI Materials and Methods*) for high-sensitivity screening of large VLR libraries for specific ligand-binding clones (Fig. 1 *B* and *C*). The display of recombinant proteins on the surface of *Saccharomyces cerevisiae* was developed as a high-throughput eukaryotic platform

Table 1. VLR affinity measured by YSD antigen titration, ITC, and SPR

Clone	YSD $K_D \pm$ SE, nM	ITC $K_D \pm$ E, nM*	SPR $K_D \pm$ SE, nM
VLRB.HEL.2D	659 ± 42	427 ± 36	455 ± 1
VLRB.2DMut.12	6.9 ± 0.2	28 ± 2	4.3 ± 0.13
VLRB.2DMut.13	ND	34 ± 3	55.1 ± 6.8
VLRB.2DMut.15	ND	8 ± 1	20.2 ± 2.1
VLRB.HEL.1	ND	602 ± 58	155 ± 19
VLRB.CTMut.5	ND	ND	0.119 ± 0.005
VLRB.HEL.21	ND	685 ± 41	117 ± 18
VLRB.Bg.1	0.03 ± 0.01	ND	0.0034 ± 0.0011
VLRA.R2.1	0.42 ± 0.01	7 ± 1	0.182 ± 0.016
VLRA.R2.6	5.6 ± 0.7	16 ± 2	1.73 ± 0.15
VLRA.R3.1	17.6 ± 2.3	129 ± 12	10.2 ± 1.0
VLRA.R4.9	20.1 ± 2.6	ND	8.38 ± 0.49
VLRA.R5.1	0.267 ± 0.015	3.5 ± 0.6	0.124 ± 0.08

SE, standard error of triplicate samples; E, uncertainties of fit; ND, not determined.
*For all ITC measurements, molar stoichiometries (*n* values) ranged from 0.94 to 1.14.

that features oxidative protein-folding machinery, glycosylation, and an efficient secretory pathway (15). Our initial experiments indicated that VLR diversity regions could be displayed C-terminally anchored on the yeast surface, with the N-termini free. In our pYSD2 vector, VLRs were fused to residues 1086–1537 from yeast flocculation protein Flo1p, which has a stalk-like structure and a C-terminal GPI cell surface anchorage motif (16) that can be used to display recombinant proteins on the surface of yeast (17). The N-terminally displayed VLRs were separated from the Flo1p anchor by a spacer that encoded a hemagglutinin (HA) tag, which served to quantify the level of surface VLR via Alexa 488-conjugated antibodies, using a fluorescence activated cell sorter (FACSort; BD Biosciences). Test ligands were biotinylated, and those bound by yeast were detected by R-phycoerythrin (RPE)-conjugated streptavidin (SAPE). The VLR–antigen complexes appear as double-positive cells in the upper-right quadrants of the dot plots (Fig. 1*D*).

VLR diversity regions were expressed on the surface of yeast as monomers at 2.5–10 $\times$ 10^3 copies per cell, as determined by FACS with reference beads (QuantiBRITE PE; BD Biosciences). Although the surface density of Flo1p fusions is lower than the density of 1–10 $\times$ 10^4 Aga2p fusions in the traditional YSD system (15), as shown below, libraries displaying VLR–Flo1p fusions can be efficiently screened for binders of both monovalent and polyvalent antigens. This indicates sufficient proximity of VLRs on the yeast surface to allow for cooperative binding of multivalent antigens by several VLRs, creating an avidity effect.

Monoclonal VLRB. We constructed VLRB YSD libraries (see *SI Materials and Methods*) from lymphocyte cDNA of HEL-immunized larvae (8×10^6 clones) and adults (6×10^7 clones) and screened both libraries for HEL binders (Fig. 1*D*). An initial enrichment by magnetic-activated cell sorting (MiniMACS; Miltenyi), with biotin-HEL and antibiotin magnetic beads, was followed by 2 successive rounds of FACS, with 5- to 7-fold enrichment of the double-positive population per round. Three clones from the larval library—VLRB.HEL.1, VLRB.HEL.2D, and VLRB.HEL.21—were selected for further analysis; all bound HEL with affinities in the range of 455–117 nM (Table 1). We calculated the affinity of VLRs for their cognate ligands from antigen titration curves produced by 3 methods. We used flow cytometry measurements of the mean fluorescence of surface-displayed VLR in a complex with SAPE-biotin-antigen, along with surface plasmon resonance (SPR), to measure the affinities of yeast-secreted biotinylated VLR (see *SI Materials and Methods*) immobilized onto NeutrAvidin-coated chips. We also measured affinity by isothermal titration calorimetry (ITC) using VLRs that were refolded in vitro from bacterial inclusion bodies. The most convenient method was antigen titration in the YSD format, which produces dissociation constants (K_D) in the same range as SPR (15, 18), whereas ITC becomes progressively less precise in the low and subnanomolar range, as discussed previously (19). Thus, we first ranked clones based on YSD antigen titrations, and then calculated dissociation constants for selected clones using all 3 methods.

To isolate binders of a broader range of antigens, we constructed a composite VLRB YSD library (4.5×10^7 clones) from lymphocyte cDNA of approximately 100 lamprey, including animals immunized with β-gal and sheep erythrocytes, and from genomic DNA of 16 lamprey extracted from whole larvae and leukocyte-rich adult livers. We then screened the composite and HEL-immunized adult libraries for binders of several multivalent antigens: β-gal (460-kDa tetramer), cholera toxin subunit B (CTB; 57-kDa pentamer), RPE (240-kDa multimer), and blood group trisaccharides A and B (≈30 kDa with 10–12 trisaccharides). The HEL-immunized adult was considered naïve with respect to all of these antigens, whereas the composite library was considered nonimmune with respect to CTB and RPE. Binders were isolated from both libraries, regardless of whether they originated from antigen-stimulated or naïve lamprey (Fig. 1*E*; Table 2). A high-avidity anti–β-gal VLRB was cloned from the composite library (K_D = 3.4 pM by SPR) and an anti-RPE VLRB from the adult library (K_D = 1.2 nM by YSD), with affinities characteristic of Ig-based single-chain antibodies isolated from immune libraries (20). Other VLRB clones bound antigens with affinities ranging from low micromolar to high nanomolar, similar to the affinities of Ig-based antibodies isolated from naïve libraries. Of the 7 trisaccharide binders that we characterized, 6 clones had 1.6- to 4.3-fold higher affinity for B-trisaccharide than for A-trisaccharide, which differs from B-trisaccharide only in the C3 saccharide, an *N*-acetylgalactosamine instead of galactose. To further test the ligand specificity of these carbohydrate-binding VLRB clones, we ran antigen titration assays for trisaccharides A or B in the presence of 10-fold excess H-trisaccharide, the basic O-antigen that lacks a C3-linked saccharide. H-trisaccharide did not inhibit binding of the cognate ligands, indicating the high specificity of these clones.

Affinity Maturation In Vitro. For biomedical applications, the affinity of Ig-based antibodies for their ligands can be improved by in vitro mutagenesis, a process resembling in vivo affinity maturation by somatic hypermutation in jawed vertebrates (20). No such data are available for any member of the LRR protein superfamily, however. Because no high-affinity anti-HEL VLRB could be isolated directly

IMMUNOLOGY

Table 2. Antigen specificity of VLRB clones

Antigen	Number of clones	Immune library, yes/no	Affinity by YSD, nM
HEL	4	Yes	400–700
B-trisaccharide	4	Yes	10–400
A/B-trisaccharide	1	No	110
B-trisaccharide	2	No	50, 900
CTB	3	No	800–10,000
β-galactosidase	1	Yes	0.03
β-galactosidase	1	No	300
R-phycoerythrin	1	No	1.17

from our libraries, we tested the feasibility of improving the affinity of VLRB.HEL.2D, the clone with the lowest affinity among the anti-HEL VLRB clones (K_D = 455 nM; Table 1 SPR). We used error-prone PCR to introduce an average of 2.8 residue substitutions along the 167-codon diversity region of VLRB.HEL.2D, and constructed a mutant YSD library (2×10^6 clones). The best HEL binders from this library were enriched by 2 FACS rounds, resulting in 5 unique clones (Fig. 2*A*) with improved affinity for HEL compared with wild-type VLRB.HEL.2D (K_D = 55–4.3 nM; Table 1 SPR), which for clone VLRB.2DMut.12 represented a 100-fold improvement.

Interestingly, all of these VLRB.HEL.2D mutants had 1 or 2 substitutions in the hypervariable loop region of LRRCT, a distinctive insert following the α-helix of this LRR module that is uniquely shared by the lamprey and hagfish VLRs and the von Willebrand factor receptor GpIbα (6). Our prediction that the hypervariable loop can contribute to antigen binding was recently validated by the crystal structure of VLRB.HEL.2D bound to HEL (21). The LRRCT loop plays a major role in this complex, where it penetrates deep into the active site cleft of the enzyme. Analysis of 517 unique VLRB sequences revealed 115 unique LRRCT loop peptides (22%); thus, we attempted to improve affinities of VLRB clones by swapping the LRRCT loop region with corresponding PCR amplicons from a large pool of VLRB cDNA. We simultaneously swapped the LRRCT loop in 4 wild-type HEL-binding clones, and constructed a mutant YSD library (2×10^7 clones) and then enriched it for improved binders by 2 rounds of MACS and 1 round of FACS (Fig. 2*B*). One of the resulting isolates was VLRB.CTMut.5, a clone derived from VLRB.HEL.1 with 6 residue substitutions in the LRRCT module, 3 of which were in the loop region (Fig. 2*C*). There were also 5 substitutions in the LRRNT-LRR1 region, which were derived from clone VLRB.HEL.2D, apparently by recombinational domain swapping during one of the overlap extension PCR reactions. Remarkably, the affinity of clone VLRB.CTMut.5 improved 1,300-fold, from 155 nM to 119 pM, during a single cycle of in vitro affinity maturation (Fig. 2*D*; Table 1 SPR), whereas 4 cycles of mutagenesis and enrichment were required for an 1,800-fold improvement of the best reported affinity-matured antifluorescein antibody (22). This indicates that a small number of residue substitutions can readily convert low-affinity monomeric VLRB into high-affinity antibodies comparable to the highest-affinity IgG.

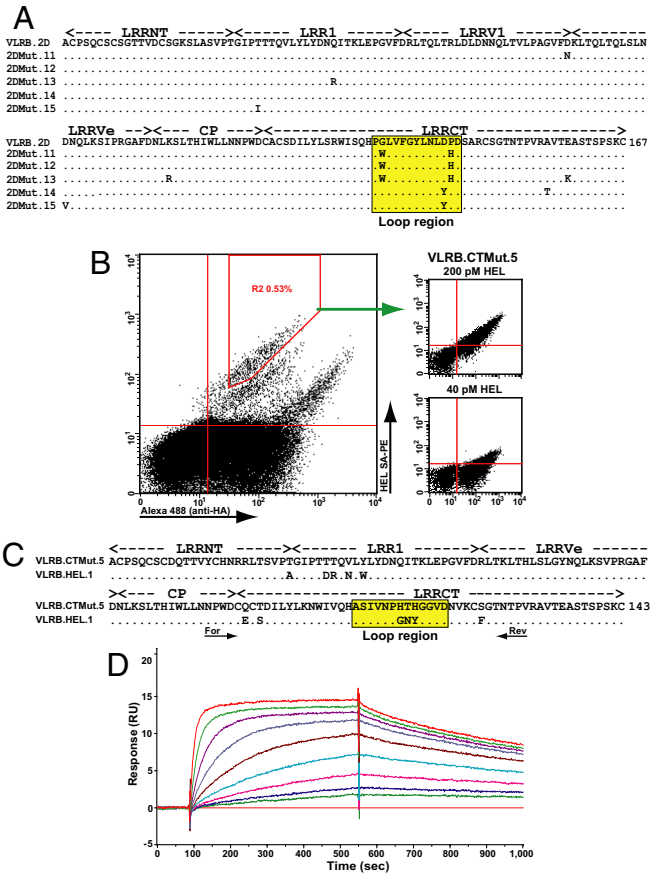

Fig. 2. Affinity maturation in vitro of VLRB antibodies. (*A*) The sequence of VLRB.HEL.2D aligned with 5 mutant clones selected after in vitro random mutagenesis. Dots indicate identity to the top sequence. The LRRCT hypervariable loop region is shaded yellow. (*B*) Sorting LRRCT loop-swapped mutants. The second MACS output was labeled with 1 nM HEL, and a representative mutant clone VLRB.CTMut.5 was stained with HEL as indicated. (*C*) The sequence of VLRB.HEL.1 aligned with mutant clone VLRB.CTMut.5. The swapped LRRCT region is delineated by PCR primers (forward, reverse). (*D*) SPR sensogram of the interaction between immobilized NeutrAvidin-biotin-VLRB.CTMut.5 with 2-fold HEL serial dilutions (7.66–0.00299 nM). K_D = 119 pM. RU, resonance units.

Monoclonal VLRA. The lamprey VLRA was discovered only recently (6), and no information on its antigen-binding properties is available. To access the VLRA repertoire, we constructed a VLRA YSD library from the HEL-immunized adult lamprey (5×10^7 clones) and screened it for HEL binders. After 2 MACS rounds, a heterogeneous cell population stained brightly with HEL at 20 nM (Fig. 3*A*). Of the 50 clones analyzed, 14 had unique nucleotide sequences, 13 of which encoded unique proteins (Fig. 3*B*). Interestingly, these 13 VLRA clones differed at only 22 out of 732 nucleotide positions, which affected 15 variable codon positions along the 244-residue diversity region. The 1.46-fold overabundance in nonsynonymous over synonymous residue substitutions may indicate that these proteins diverged under positive selection, as further suggested by the nearly 100-fold augmentation, from 26 nM to 270 pM, in ligand-binding affinity among these VLRAs (Fig. 3*C* and *D*). To determine whether these mature VLRA genes were mutated in the lamprey lymphocytes or whether mutations were uninten-

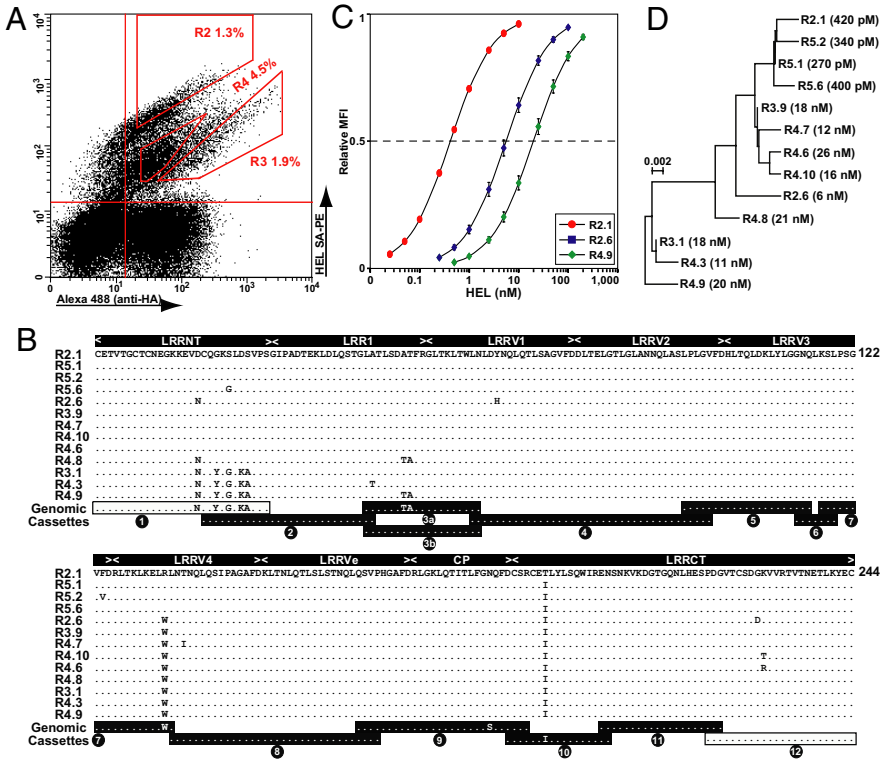

Fig. 3. Monoclonal VLRA antibodies cloned from a HEL-immunized adult lamprey. (*A*) Sorting anti-HEL VLRA. The second MACS output was labeled with 20 nM HEL. Clones were sorted using gates R2–R4. (*B*) Protein sequence alignment of 13 anti-HEL VLRA; only residues 3–246 are shown. Tiled below: germline *VLRA* gene portions (boxes 1 and 12) and the corresponding genomic LRR cassettes (boxes 2–11; 3a and 3b alternative cassettes). Dots indicate identity to the top sequence. (*C*) VLRA YSD antigen titrations. Normalized mean fluorescence intensity of biotin-HEL-SAPE plotted against 2-fold serial HEL dilutions (for R2.1, 10−0.025 nM; for R2.6, 100−0.25 nM; for R4.9, 200−0.5 nM). Bars indicate SEs of triplicate samples. (*D*) Neighbor-joining tree of the VLRA nucleotide sequences. The corresponding K_D values calculated by YSD antigen titration are given in parentheses.

tionally introduced during YSD library construction, we compared the sequences of YSD VLRAs to PCR-amplified clones from the same lymphocyte cDNA sample. The distribution of variable nucleotide and residue substitutions was similar among the VLRAs selected by YSD and the unselected PCR clones (Fig. S2), indicating that these mutations occurred in the lamprey lymphocytes.

We have previously shown that lamprey VLRs are assembled from flanking genomic LRR-encoding cassettes via a gene conversion–like process (6). Here we used the same method to search for "footprints" of gene conversion among the variant VLRA clones by tiling the corresponding portions of germline *VLRA* genes and genomic LRR cassettes along the mature VLRA sequences. Several potential recombination events were evident; for example, the LRRNT of clones R4.8, R3.1, R4.3, and R4.9 was identical to the germline gene portion (Fig. 3*B*, box 1), whereas in all other sequences, the C-terminal half of LRRNT was identical to genomic cassette 2 at all 6 variant nucleotides. In the region corresponding to cassette 3, 4 nucleotides distinguished cassette 3a from cassette 3b; clone R4.9 was identical to cassette 3a, and clone R4.8 had 3 of the 4 unique nucleotides of cassette 3a, whereas all other clones had sequences identical to cassette 3b in this region. The simultaneous substitution of clusters of codons in these mature VLRA genes (4 in LRRNT and 2 in LRR1) is consistent with a process of gene conversion between the mature VLRA gene and 1 or more of the VLRA genomic LRR cassettes. Thus, these variant VLRAs appear to be derived from a single lymphocyte progenitor, which has a mature VLRA gene most closely to the sequence of VLRA.R4.9 in our sample. Interestingly, a phylogenetic neighbor-joining tree (23) drawn for the VLRA sequences clustered all of the subnanomolar HEL-binding clones (R2.1, R5.1, R5.2, and R5.6) based on a single substitution of the hydrophobic tryptophan at position 136 to a charged hydrophilic arginine. Alignment of these VLRA sequences based on the available VLR structures revealed that residue 136 is located at a solvent-exposed position in the LRRV4 β-strand, which is part of the concave antigen-binding surface of VLRs (12, 21).

Thus, VLRA antibodies are capable of very high-affinity interactions with antigens. For instance, the best VLRA HEL-binding clone (R5.1) had a K_D of 124 pM, approaching the 100 pM affinity ceiling of Ig-based antibodies produced during mammalian immune responses (1, 24). Future studies will address the question of whether these VLRA variants arose as part of the primary repertoire, as in sheep and rabbits (25, 26), or as a consequence of antigen-driven affinity maturation of antibody responses, as in all jawed vertebrates from shark to man (2).

In conclusion, the powerful YSD platform described herein has allowed us to explore the role of VLR in lamprey immunity by screening large libraries for specific antigen-binding VLR clones. After conversion to VLR display via the C-terminal Flo1p anchor, the optimized system allowed highly sensitive library screening for clones with binding affinities, or avidities, in the range of 10^{-6} to 10^{-12} M. The broad spectrum of antigens that VLR can specifically recognize, including monovalent and multivalent proteins and saccharides, and the binding affinities achieved, clearly attest to the remarkable diversity of the VLR repertoire in both naïve and antigen-stimulated lamprey. This suggests that the naïve VLRB repertoire includes at least low-affinity binders of many antigens. The monomeric YSD VLRB diversity regions that we assayed actually could have been derived from native high-avidity multimeric VLRB binders of these antigens. Furthermore, our analysis of anti-HEL VLRA

variants and in vitro matured VLRB clones has shown that mutations can significantly enhance the affinities of these LRR-based adaptive immune receptors. Thus, the VLR system of jawless vertebrates truly behaves like the Ig-based system of jawed vertebrates, with the potential to provide an effective humoral antipathogen shield.

VLRs also hold considerable potential as natural non-Ig antibodies for various biotechnology applications (27, 28). These highly stable modular single-chain polypeptides of relatively small size (15–25 kDa) can bind a broad range of antigenic determinants with high affinity and specificity, and can be readily engineered for improved binding properties. VLR antibodies could serve in such diagnostic applications as biosensors, bioimaging, flow cytometry, immunohistochemistry, and ELISA, as well as in affinity purification. In addition, lamprey VLR may provide a rich source of reagents that recognize mammalian antigens invisible to Ig-based antibodies because of self-tolerance.

Materials and Methods

YSD Library Screening. Libraries were enriched for antigen-binding clones by 1 or 2 rounds of MACS using 0.5–1 μM biotinylated antigen, antibiotin microbeads, and a MiniMACS separation unit (Miltenyi). The wash buffer consisted of PBS, 0.5% BSA, 2 mM EDTA, and 0.1% Tween 20. Propagated MACS output cells were enriched by 1–3 rounds of FACS, labeled with 2–500 nM biotinylated antigen and 100 ng/mL of rat anti-HA (clone 3F10; Roche). The cells were rotated for 25 min at room temperature and then placed on ice for 5 min. Cells were washed 3 times and incubated with 1:200 dilutions of Alexa Fluor-488 donkey anti-rat IgG (Invitrogen) and SAPE (Invitrogen) for 20 min on ice. Cells were then washed 3 times with PBS and 0.1% BSA, and then sorted using a FACSort equipped with a cell concentration module (BD Biosciences).

VLRB In Vitro Mutagenesis. The VLRB.HEL.2D amplicon at 15 ng/μL was diluted 7,000-fold, and 1 μL was used as a template for PCR using a GeneMorph II kit (Stratagene). Average residue substitutions were determined from 16 mutagenized clones. To swap the LRRCT loop region, the VLRB 5′ region, from LRRNT to CP, was amplified with primers LRRNTS.F 5-GCATGTCCCTCGCA and CP.R 5-CAGTCCCAGGGGTT. The hypervariable loop region (112–148 bp) was amplified from pooled VLRB amplicons using primers CP.F 5-AACCCCTGGGACTG and 3LRRCT.R 5-GGACGGGGGTATTG (Fig. 2*C*). The resulting amplicons were assembled by overlap extension PCR using primers LRRNT.F 5-GCATGTCCCTCGCAGTGTTC and LRRCT.R 5-TGGGCATTTCGAGGGGCTAGTGCTGGCCTCGGTGACCGCACGGACGGGGGTATTG. The resulting amplicons were amplified with primers VLRB.F+VLRB.R and cloned in pYSD2.

Equilibrium Dissociation Constants. YSD antigen titrations of VLRs were performed as described previously (18). Triplicate aliquots of 10^5 yeast cells were labeled with antigen concentrations ranging from 10-fold above to 10-fold below the dissociation constant. Equilibrium dissociation constants were obtained by plotting total mean fluorescence (PE channel) against antigen concentration, using nonlinear least squares to fit the curve. A BIAcore T100 biosensor (GE Healthcare) was used for affinity analysis of VLR–ligand interactions. Secreted biotinylated VLRs were desalted (HiTrap column; GE Healthcare) and captured onto NeutrAvidin (Pierce) amine-coupled to a CM5 chip (GE Healthcare). Analytes were injected at 40 μL/min in HBS-EP buffer (GE Healthcare). Immobilized VLRs were regenerated by injection of 10 mM glycine-HCl (pH 2) and 0.005% Tween at 10 μL/min for 20 s. SPR data were fitted to a predefined 1:1 kinetic binding model to obtain the on and off rates.

For ITC measurements, VLRs were cloned in pT7–7 (Novagen), and expressed as inclusion bodies in *Escherichia coli* BL21-CodonPlus(DE3)-RIL (Stratagene). Induced bacteria were sonicated in 50 mM Tris-HCl (pH 8), 0.1 M NaCl, and 2 mM EDTA. Inclusion bodies were washed with 50 mM Tris-HCl (pH 8), 0.1 M NaCl, and 0.5% (vol/vol) Triton X-100, then solubilized in 8 M urea and 100 mM Tris-HCl (pH 8.5). Proteins were diluted to 10 mg/L with 0.8 M arginine, 100 mM Tris-HCl (pH 8.5), 2 mM EDTA, 3 mM reduced glutathione, and 0.3 mM oxidized glutathione. After 3 days at 4 °C, folding mixtures were concentrated, dialyzed against 20 mM Tris-HCl (pH 8.5), and applied to a MonoQ column (GE Healthcare). A Superdex 75 HR column (GE Healthcare) was used for purification. ITC measurements were carried out at 25 °C in a MicroCal VP-ITC unit (GE Healthcare). Purified VLRs and HEL were dialyzed against 5 mM phosphate (pH 7.2), 136 mM NaCl, and 4 mM KCl. Typically, 3-μL aliquots of 0.638–3.95 mM HEL were injected from a 250-μL syringe rotating at 290 rpm into the sample cell containing 1.37 mL of 0.025–0.060 mM VLR solution. Corrections for buffer dilution were subtracted from the binding data. K_D values were calculated by nonlinear least squares fits of ITC data for a single-site binding model. Data were acquired and analyzed using ORIGIN software.

ACKNOWLEDGMENTS. We thank F.J. Chrest (Johns Hopkins) and D. Nance (University of Maryland, Baltimore) for assistance with sorting, M.B. Murphy (GE Healthcare) for advice on SPR, and M.C. Kerzic (Center for Advanced Research in Biotechnology) for technical assistance. This work was supported by National Science Foundation Grant MCB-0614672 (to Z.P.), National Institutes of Health Grants AI065612 and AI036900 (to R.A.M.), and a University of Maryland Biotechnology Institute Intercenter Collaboration Grant (to Z.P. and R.A.M.).

1. Batista FD, Neuberger MS (1998) Affinity dependence of the B cell response to antigen: A threshold, a ceiling, and the importance of off-rate. *Immunity* 8:751–759.
2. Dooley H, Stanfield RL, Brady RA, Flajnik MF (2006) First molecular and biochemical analysis of in vivo affinity maturation in an ectothermic vertebrate. *Proc Natl Acad Sci USA* 103:1846–1851.
3. Pancer Z, et al. (2004) Somatic diversification of variable lymphocyte receptors in the agnathan sea lamprey. *Nature* 430:174–180.
4. Pancer Z, et al. (2005) Variable lymphocyte receptors in hagfish. *Proc Natl Acad Sci USA* 102:9224–9229.
5. Alder MN, et al. (2005) Diversity and function of adaptive immune receptors in a jawless vertebrate. *Science* 310:1970–1973.
6. Rogozin IB, et al. (2007) Evolution and diversification of lamprey antigen receptors: Evidence for involvement of an AID-APOBEC family cytosine deaminase. *Nat Immunol* 8:647–656.
7. Pancer Z, Cooper MD (2006) The evolution of adaptive immunity. *Annu Rev Immunol* 24:497–518.
8. Alder MN, et al. (2008) Antibody responses of variable lymphocyte receptors in the lamprey. *Nat Immunol* 9:319–327.
9. Nagawa F, et al. (2007) Antigen-receptor genes of the agnathan lamprey are assembled by a process involving copy choice. *Nat Immunol* 8:206–213.
10. Kim HM, et al. (2007) Structural diversity of the hagfish variable lymphocyte receptors. *J Biol Chem* 282:6726–6732.
11. Herrin BR, et al. (2008) Structure and specificity of lamprey monoclonal antibodies. *Proc Natl Acad Sci USA* 105:2040–2045.
12. Han BW, Herrin BR, Cooper MD, Wilson IA (2008) Antigen recognition by variable lymphocyte receptors. *Science* 321:1834–1837.
13. Sundberg EJ, Mariuzza RA (2003) Molecular recognition in antigen–antibody complexes. *Adv Protein Chem* 61:119–160.
14. Stanfield RL, Dooley H, Flajnik MF, Wilson IA (2004) Crystal structure of a shark single-domain antibody V region in complex with lysozyme. *Science* 305:1770–1773.
15. Chao G, et al. (2006) Isolating and engineering human antibodies using yeast surface display. *Nat Protoc* 1:755–768.
16. Teunissen AW, Holub E, van der Hucht J, van den Berg JA, Steensma HY (1993) Sequence of the open reading frame of the FLO1 gene from *Saccharomyces cerevisiae*. *Yeast* 9:423–427.
17. Sato N, et al. (2002) Long anchor using Flo1 protein enhances reactivity of cell surface–displayed glucoamylase to polymer substrates. *Appl Microbiol Biotechnol* 60:469–474.
18. Feldhaus MJ, et al. (2003) Flow-cytometric isolation of human antibodies from a nonimmune *Saccharomyces cerevisiae* surface display library. *Nat Biotechnol* 21:163–170.
19. Velázquez-Campoy A, Freire E (2005) ITC in the post-genomic era? Priceless. *Biophys Chem* 115:115–124.
20. Wark KL, Hudson PJ (2006) Latest technologies for the enhancement of antibody affinity. *Adv Drug Delivery Rev* 58:657–670.
21. Velikovsky CA, et al. (2009) Structure of a lamprey variable lymphocyte receptor in complex with a protein antigen. *Nat Struc Mol Biol* 16:725–730.
22. Boder ET, Midelfort KS, Wittrup KD (2000) Directed evolution of antibody fragments with monovalent femtomolar antigen-binding affinity. *Proc Natl Acad Sci USA* 97:10701–10705.
23. Kumar S, Tamura K, Nei M (2004) MEGA3: Integrated software for molecular evolutionary genetics analysis and sequence alignment. *Brief Bioinform* 5:150–163.
24. Foote J, Eisen HN (1995) Kinetic and affinity limits on antibodies produced during immune responses. *Proc Natl Acad Sci USA* 92:1254–1256.
25. Becker RS, Knight KL (1990) Somatic diversification of immunoglobulin heavy- chain VDJ genes: Evidence for somatic gene conversion in rabbits. *Cell* 63:987–997.
26. Reynaud CA, Garcia C, Hein WR, Weill JC (1995) Hypermutation generating the sheep immunoglobulin repertoire is an antigen-independent process. *Cell* 80:115–125.
27. Binz HK, Amstutz P, Plückthun A (2005) Engineering novel binding proteins from nonimmunoglobulin domains. *Nat Biotechnol* 23:1257–1268.
28. Skerra A (2007) Alternative non-antibody scaffolds for molecular recognition. *Curr Opin Biotechnol* 18:295–304.